

Frédéric Roger

# Analysis of magnetohydrodynamics GTAW arc behavior

**Abstract** Argon plasma behavior in gas tungsten arc welding (GTAW) is directly linked to the weld quality. Indeed, the arc is the heat source which drives the weld shape. Solution of an induction-diffusion equation under axial symmetry conditions has been developed using thermal conduction and convection module of Femlab 3.1©. We predict current distribution in electric arc, induced magnetic field and then resulting electromagnetic forces.

The latter is introduced in incompressible axial symmetric Navier-Stokes equations. Both Pdes are strongly coupled. Indeed, Plasma velocity field introduces a source term in the induction diffusion equation.

**Keywords** Arc welding – magnetohydrodynamics - plasma

## 1 Introduction

The first work about electromagnetic arc plasma behavior is fifty years old [1] with the Maecker's description of the convection in the plasma which is assumed to be in local thermodynamic equilibrium (LTE) with the same local temperature for ions and electrons.

Convection, with high plasma velocity (about 100m/s), drives heat transfer with the weld pool and then the shape and the thermomechanics behavior of the weld.

Femlab allows to consider the whole set of non linear physics equations (non linear coupling PDE's) to describe the velocity, the temperature and the electromagnetic field in the arc plasma. In the present work we describe the strong coupling between flow field and induced electromagnetic field. For this purpose, axial symmetric two dimensional Navier Stokes and induction-convection equations are solved simultaneously.

## 2 Mathematical model

The model describes the fluid flow and the electromagnetic field in the space between the tungsten cathode and the anode workpiece. We consider an axial symmetric two dimensional description.

The 2D axial symmetric stationary Navier Stokes incompressible equations are used in Femlab 3.1 fluid dynamics module. For the convection induction equation, we use the conductive and convective stationary heat transfer model. Temperature T is then replaced by the azimuthal magnetic field  $B_\theta$ .

### 2.1 Governings equations

We consider the magnetic field B as the principal electromagnetic quantity. All the other quantities ( $\mathbf{E}, \mathbf{J}, \mathbf{q}$ ) can be deduced using Maxwell's equations and Ohm's Law. From Ohm's law, Ampere and Faraday's equations we can deduce the stationary induction convection equation :

$$\text{curl}(\mathbf{u} \wedge \mathbf{B}) + \frac{1}{\mu\sigma} \Delta \mathbf{B} = 0 \quad (1)$$

with  $\mathbf{u}$  the plasma velocity ( $\text{m.s}^{-1}$ ),  $\mu$  the permeability of matter (or vacuum,  $\text{H.m}^{-1}$ ) and  $\sigma$  the electrical conductivity ( $\Omega^{-1}.\text{m}^{-1}$ ).

In the 2D axial symmetric configuration, equation (1) becomes :

$$\frac{1}{\mu\sigma} \Delta B_\theta - \mathbf{u} \cdot \nabla B_\theta - B_\theta \left( \frac{\partial u_z}{\partial z} + \frac{\partial u_r}{\partial r} + \frac{1}{\mu\sigma r^2} \right) = 0 \quad (2)$$

Equation (2) is similar to stationary conduction-convection heat transfer equation with an heat source term.

The fluid flow is described by 2D axial symmetric stationary incompressible Navier Stokes equations :

$$\begin{aligned} \rho(\mathbf{u} \cdot \nabla) \mathbf{u} &= \nabla \cdot (-p\mathbf{I} + \eta(\nabla \mathbf{u} + (\nabla \mathbf{u})^t)) + \mathbf{J} \wedge \mathbf{B} \\ \nabla \cdot \mathbf{u} &= 0 \end{aligned} \quad (3)$$

with  $\eta$  the dynamical viscosity ( $\text{kg} \cdot \text{m}^{-1} \cdot \text{s}^{-1}$ ),  $\mathbf{J}$  the current density ( $\text{A} \cdot \text{m}^{-2}$ ).

The Lorentz electromagnetic force  $\mathbf{J} \wedge \mathbf{B}$  is a volumic force ( $\text{N} \cdot \text{m}^{-3}$ ).  $\mathbf{J}$  is deduced from  $\mathbf{B}$  with the help of the Maxwell equation.

$$J_r = \frac{1}{\mu} \frac{\partial B_\theta}{\partial z} \quad (4)$$

$$J_z = \frac{1}{\mu r} \frac{\partial}{\partial r} (r B_\theta) \quad (5)$$

## 2.2 Calculation domain and boundary conditions

The computational domain is illustrated in Fig 1. FE is the cathode spot region, ED is the inflow argon region and AF is the symmetry axis. The arc length AF is 6.3 mm.

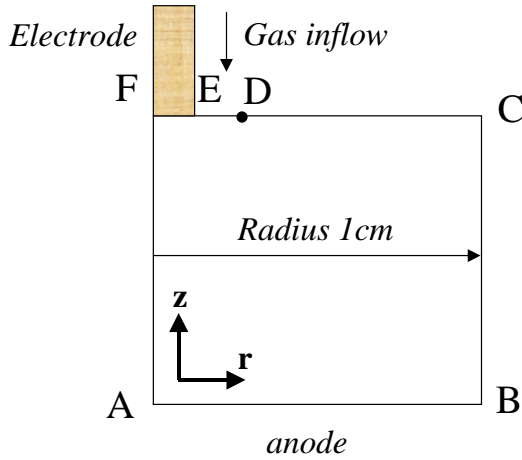


Fig 1. Arc column calculation domain

Boundary conditions are specified in Table 1 where  $R_c$  is the electrode radius (1.2mm),  $I$  is the welding current (300A),  $\mu_0$  is the permeability of vacuum ( $4\pi \cdot 10^{-7} \text{H} \cdot \text{m}^{-1}$ ).

A-B	$u_r = 0, u_z = 0$	$\partial B_\theta / \partial z = 0$
B-C	$P = 10^5 \text{ Pa}$	$\partial B_\theta / \partial r = 0$
C-D	$P = 10^5 \text{ Pa}$	$B_\theta = \mu_0 I / 2\pi r$
D-E	$u_z = -10 \text{ m/s}, u_r = 0$	$B_\theta = \mu_0 I / 2\pi r$
E-F	$u_r = 0, u_z = 0$	$B_\theta = \mu_0 I r / 2\pi R_c^2$
A-F	$u_r = 0, \partial u / \partial z = 0$	$B_\theta = 0$

Table 1. Boundary conditions for the arc model

The material properties of argon plasma are constants and are taken from the references [2,3].

## 3 Results

### 3.1. Magnetic field distribution

The results of the simulation are represented in Fig 2 which displayed the calculated magnetic field with 300 A arc current. The intensity of the magnetic field is maximal near the cathode spot (point E in fig 1) and decrease at the plasma centerline near the anode spot (point A in fig 1). The effect of this distribution is a maximum Lorentz force ( $\mathbf{J} \times \mathbf{B}$ ) near the gas inflow and then a high acceleration of the flow (pumping). The maximum magnetic field near the point E is 0.05 T.

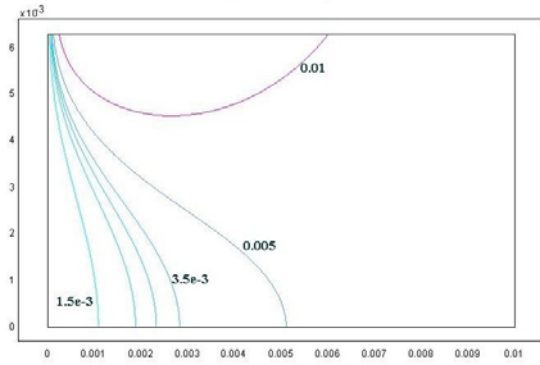


Fig 2. :  $B_\theta$  field isovalues

### 3.2. Fluid flow distribution

Fig 3. shows the distribution of flow field in the plasma for a 300 A welding current. Plasma flows from the gas inflow to anode spot along the plasma centerline. The simulation in this investigation neglected the effect of turbulence.

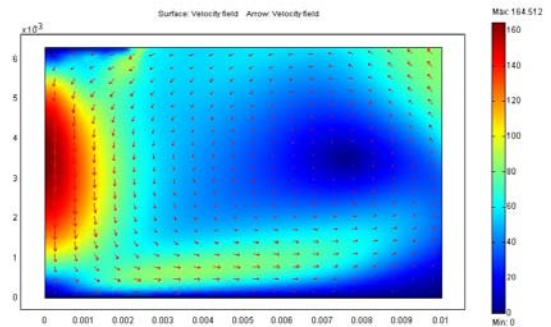
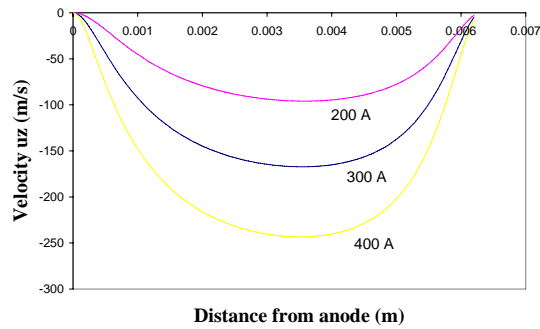


Fig 3. Velocity field (m/s) in the plasma

Fig 4 shows the axial velocity distribution along the plasma centerline for three different welding currents (200, 300 and 400A). The maximum velocity is located near the middle of the centerline and is

repectively 96, 164 and 243 m/s for the 200, 300 and 400 A welding current. This distribution have a good agreement with the works of M. A. Ramirez with a bell like shape [4].



*Fig 4. Axial velocity at the symmetry line for 200, 300 and 400 A welding current*

#### 4 Conclusions

A mathematical model of the MHD behavior of the arc plasma was constructed using Femlab multiphysics's ability. The strong coupling between fluid flow and magnetic field was developed for a axial symmetry configuration. For this purpose, an induction-convection model has been introduced. Fluid flow results are in good agreement with the litterature [4].

#### References

1. C. W. Chang et al, The modelling of gas velocity fields in welding arcs, Arc physics and weld pool behavior, The welding Institute, Cambridge, Eng, 381 (1980).
2. H.G Fan, Y.W. Shi, Numerical simulation of the arc pressure in gas tungsten arc welding, 302-308. Journal of Materials Processing Technology 61, (1996).
3. M. Tanaka, M. Ushio, J.J. Lowke, Numerical study of gas tungsten arc plasma with anode melting, 381-389. Vacuum 73, (2004).
4. M. A. Ramirez, G. Trapaga, J McKelliget, A comparison between different numerical formulations for welding arc representations, 1634-1640. Journal of Materials Processing Technology 155-156, (2004).